

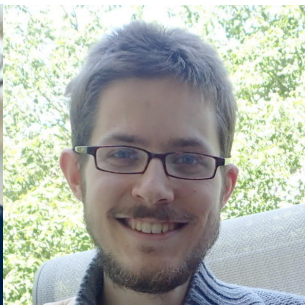
# BPS Dendroscopy on Local Projective Plane

Boris Pioline



"Intersections of Strings and QFT IV"  
Birmingham, 8/9/2023

# My amazing co-authors



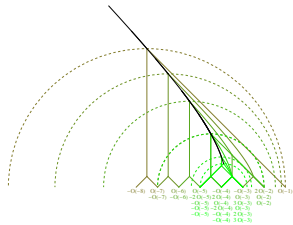
*Based on 'BPS Dendroscopy on Local  $\mathbb{P}^2$ ' [2210.10712]  
with Pierrick Bousseau, Pierre Descombes and Bruno Le Floch*



Dentology



Dendrochronology



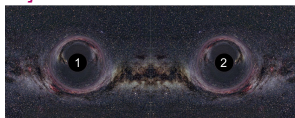
Dendrosocopy

- In type IIA string theory compactified on a Calabi-Yau threefold  $X$ , the BPS spectrum consists of bound states of **D6-D4-D2-D0 branes**, with charge  $\gamma \in H_{\text{even}}(X, \mathbb{Q})$ .
- BPS states saturate the bound  $M(\gamma) \geq |Z(\gamma)|$ , where the central charge  $Z \in \text{Hom}(\Gamma, \mathbb{C})$  depends on the complexified **Kähler moduli**.
- The index  $\Omega_z(\gamma)$  counting BPS states is robust under complex structure deformations, but in general depends on  $z \in \mathcal{M}_K$ .
- Mathematically, the **Donaldson-Thomas invariant**  $\Omega_z(\gamma)$  counts stable objects with  $\text{ch } E = \gamma$  in the **derived category of coherent sheaves**  $\mathcal{C} = D^b\text{Coh}(X)$ .



# Introduction

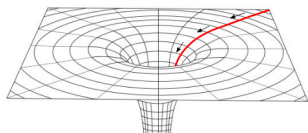
- $\Omega_Z(\gamma)$  is locally constant on  $\mathcal{M}_K$ , but can jump across real codimension one **walls of marginal stability**  $\mathcal{W}(\gamma_L, \gamma_R) \subset \mathcal{M}_K$ , where the phases of the central charges  $Z(\gamma_L)$  and  $Z(\gamma_R)$  with  $\gamma = m_L \gamma_L + m_R \gamma_R$  become aligned [*Kontsevich Soibelman'08, Joyce Song'08*]
- Physically, **multi-centered black hole solutions with charges**  $\gamma_i = m_{L,i} \gamma_L + m_{R,i} \gamma_R$  (dis)appear across the wall [*Denef'02, Denef Moore '07, ..., Manschot BP Sen '11*].



$$\frac{\langle \gamma_L, \gamma_R \rangle}{r} = \frac{2 \operatorname{Im}[\bar{Z}(\gamma_L) Z(\gamma_R)]}{|Z(\gamma_L + \gamma_R)|}, \quad \Delta \Omega(\gamma) = \pm |\langle \gamma_L, \gamma_R \rangle| \Omega(\gamma_L) \Omega(\gamma_R)$$

- These multi-centered bound states are expected to decay away as one follows the attractor flow equations [*Ferrara Kallosh Strominger'95*]

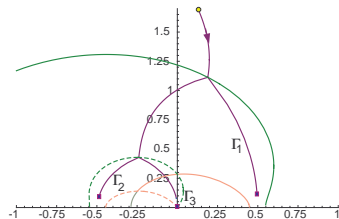
$$\text{AF}_\gamma : \quad r^2 \frac{dz^a}{dr} = -g^{a\bar{b}} \partial_{\bar{b}} |Z_z(\gamma)|^2$$



- Let  $z_*(\gamma)$  be the endpoint of the flow, or **attractor point**. Since  $Z_z(\gamma)$  decreases along the flow,  $z_*(\gamma)$  can either be a regular local minimum of  $|Z_z(\gamma)|$  with  $|Z_{z_*(\gamma)}(\gamma)| > 0$ , or a conifold point if  $Z_{z_*(\gamma)}(\gamma) = 0$ .
- We define the **attractor invariant** as  $\Omega_*(\gamma) = \Omega_{z_*(\gamma)}(\gamma)$ .

# The Split Attractor Flow Conjecture

- Starting from  $z \in \mathcal{M}_K$ , following  $AF_\gamma$  and recursively applying the WCF formula at whenever the flow crosses a wall of marginal stability, one can in principle express  $\Omega_z(\gamma)$  in terms of attractor invariants.



*Denef Moore'07*

# The Split Attractor Flow Conjecture (SFAC)

- In terms of the **rational DT invariants**

$$\bar{\Omega}_z(\gamma) := \sum_{k|\gamma} \frac{y^{-1/y}}{k(y^k - y^{-k})} \Omega_z(\gamma/k)_{y \rightarrow y^k}$$

the result takes the form

$$\bar{\Omega}_z(\gamma) = \sum_{\gamma = \sum \gamma_i} \frac{g_z(\{\gamma_i\})}{\text{Aut}(\{\gamma_i\})} \prod_i \bar{\Omega}_*(\gamma_i)$$

where  $g_z(\{\gamma_i\})$  is a sum over **attractor flow trees**.

- The **Split Attractor Flow Conjecture** [Denef'00, Denef Moore'07] is the statement that only a **finite** number of decompositions  $\gamma = \sum \gamma_i$  contribute to the index  $\bar{\Omega}_z(\gamma)$ .

# The Split Attractor Flow Conjecture

- Unfortunately one does not know a priori which constituents  $\gamma_i$  can contribute, except for the obvious constraints

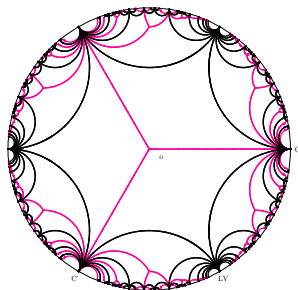
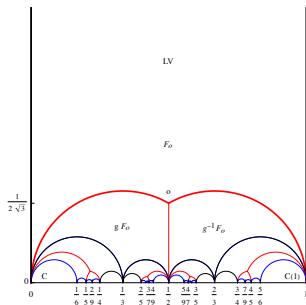
$$\sum_i \gamma_i = \gamma, \quad \sum_i |Z_{z_\star(\gamma_i)}(\gamma_i)| < |Z_z(\gamma)|$$

- In particular, there can be **cancellations between D-branes and anti-D-branes**, and contributions from **conifold states** which are massless at their attractor point are difficult to bound.
- Even if SAFC holds, one still has to compute the attractor indices  $\Omega_\star(\gamma)$ , a tall order for regular attractor points.

- Our aim is to investigate the Split Attractor Flow Conjecture for one of the simplest examples of CY threefolds, namely  $X = K_{\mathbb{P}^2} = \widetilde{\mathbb{C}^3/\mathbb{Z}_3}$  [Douglas Fiol Romelsberger'00].
- We show that the only possible constituents are the D4-brane  $\mathcal{O}_{\mathbb{P}^2}$  and anti-D4-brane  $\mathcal{O}_{\mathbb{P}^2}[1]$ , and images thereof under  $\Gamma_1(3)$ , each carrying attractor index  $\Omega_*(\gamma) = 1$ .
- In particular, in the large volume region the full BPS spectrum arises as **bound states of fluxed D4 and anti-D4-brane**, with effective bounds on the number and flux of the constituents.
- A key role is played by **scattering diagrams**, which provide the correct mathematical framework for the SAFC, at least for local CY threefolds.

# Kähler moduli space

- By local mirror symmetry, the Kähler moduli space of  $X = K_{\mathbb{P}^2}$  is the quotient  $X_1(3) = \mathbb{H}/\Gamma_1(3)$ . It admits two cusps  $LV, C$  and one orbifold point  $o$  of order 3.



- A BPS state on  $X$  is a stable object  $E$  in the bounded derived category  $\mathcal{C}$  of compactly supported sheaves on  $X$ , with charge  $\gamma(E) = \text{ch}(\pi_*(E)) = [r, d, \text{ch}_2] \sim [D4, D2, D0]$

# Central charge as Eichler integral

- The central charge  $Z_\tau(\gamma)$  is a linear combination

$$Z_\tau(\gamma) = -rT_D(\tau) + dT(\tau) - ch_2$$

where  $T_D, T$  are single-valued functions on  $\mathbb{H}$  (but not on  $\mathcal{M}_K$ ). They are periods of a one-form  $\lambda$  with logarithmic singularities on the mirror curve, satisfying a Picard-Fuchs equation of degree 3.

- It turns out that  $\partial_\tau \lambda$  is holomorphic, so its periods are proportional to  $(1, \tau)$ . Integrating along a path from  $o$  to  $\tau$ , one can establish the Eichler-type integral representation

$$\begin{pmatrix} T \\ T_D \end{pmatrix} = \begin{pmatrix} 1/2 \\ 1/3 \end{pmatrix} + \int_{\tau_0}^{\tau} \begin{pmatrix} 1 \\ u \end{pmatrix} C(u) du$$

where  $C(\tau) = \frac{\eta(\tau)^9}{\eta(3\tau)^3} = 1 - 9q + \dots$  is a weight 3 Eisenstein series for  $\Gamma_1(3)$ .



# Central charge as Eichler integral

- This provides an computationally efficient analytic continuation of  $Z_\tau$  throughout  $\mathbb{H}$ , and gives access to monodromies:

$$\tau \mapsto \frac{a\tau + b}{c\tau + d} \quad \begin{pmatrix} 1 \\ T \\ T_D \end{pmatrix} \mapsto \begin{pmatrix} 1 & 0 & 0 \\ m & d & c \\ m_D & b & a \end{pmatrix} \cdot \begin{pmatrix} 1 \\ T \\ T_D \end{pmatrix}$$

where  $(m, m_D)$  are period integrals of  $C$  from  $\tau_0$  to  $\frac{d\tau_0 - b}{a - c\tau_0}$ .

- At large volume  $\tau \rightarrow i\infty$ , using  $C = 1 + \mathcal{O}(q)$  one finds

$$T = \tau + \mathcal{O}(q), \quad T_D = \frac{1}{2}\tau^2 + \frac{1}{8} + \mathcal{O}(q)$$

in agreement with  $Z_\tau(\gamma) \sim -\int_S e^{-\tau H} \sqrt{\text{Td}(S)} \text{ch}(E)$ .

# Space of Bridgeland stability conditions

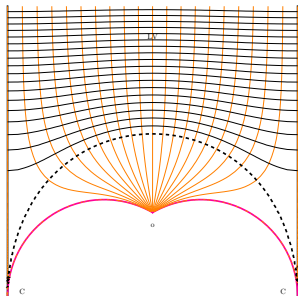
- Donaldson-Thomas invariants are defined in the larger **space of Bridgeland stability conditions**  $\text{Stab } \mathcal{C} = \{\sigma = (Z, \mathcal{A})\}$ , where  $Z : \Gamma \rightarrow \mathbb{C}$  is a linear map and  $\mathcal{A} \subset \mathcal{C}$  an Abelian category (heart of  $t$ -structure) satisfying various axioms, e.g.  $\text{Im}Z(\gamma(E)) \geq 0 \forall E \in \mathcal{A}$ .
- The group  $\widetilde{GL}(2, \mathbb{R})^+$  acts on  $\text{Stab } \mathcal{C}$  by linear transformations of  $(\text{Re}Z, \text{Im}Z)$  with positive determinant, leaving  $\Omega_\sigma(\gamma)$  invariant.
- For  $\tau_2$  large enough, one can use  $\widetilde{GL}(2, \mathbb{R})^+$  to absorb the  $1/8$  and  $\mathcal{O}(q)$  corrections to  $Z_\tau(\gamma)$  and reach the **large volume slice**

$$Z_{(s,t)}^{LV}(\gamma) = -\frac{r}{2}(s+it)^2 + d(s+it) - ch_2,$$

with  $\tau \simeq s + it$ .

# Space of Bridgeland stability conditions

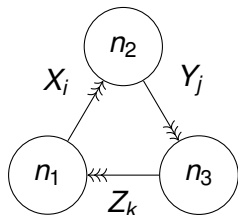
- Specifically, this holds in the region  $w > \frac{1}{2}s^2$  where  $(s, w) := \left(\frac{\text{Im}T_D}{\text{Im}T}, -\frac{\text{Im}(T\bar{T}_D)}{\text{Im}T}\right)$ . In  $(s, t = \sqrt{2w - s^2})$  plane:



- The large volume slice does not cover the region around the orbifold point, and covers only part of the conifold point.

# Quiver for $K_{\mathbb{P}^2}$

- The category  $D^b \text{Coh}_c(K_{\mathbb{P}^2})$  is isomorphic to the category of representations a quiver with potential  $(Q, W)$ , whose nodes correspond to fractional branes on  $\mathbb{C}^3/\mathbb{Z}_3$ :



$$W = \sum \epsilon_{ijk} X_i Y_j Z_k$$

$$\begin{aligned} E_1 &= \mathcal{O}[-1] & \gamma_1 &= [-1, 0, 0] \\ E_2 &= \Omega(1), & \gamma_2 &= [2, -1, -\frac{1}{2}] \\ E_3 &= \mathcal{O}(-1)[1] & \gamma_3 &= [-1, 1, -\frac{1}{2}] \end{aligned}$$

$$\begin{aligned} r &= 2n_2 - n_1 - n_3 \\ d &= n_3 - n_2 \\ \text{ch}_2 &= -\frac{1}{2}(n_2 + n_3) \end{aligned}$$

- The quiver description is valid in a region where the central charges  $Z(E_i)$  lie in a common half-plane, which includes the orbifold point  $\tau_0 = -\frac{1}{2} + \frac{i}{2\sqrt{3}}$ , where  $Z_{\tau_0}(\gamma_i) = 1/3$  for  $i = 1, 2, 3$ .

# Attractor flow tree formula for quivers

- In that region,  $\Omega_\tau(\gamma)$  coincides with the **quiver index**  $\Omega_\theta(\gamma)$  counting  **$\theta$ -semi-stable representations** of dimension vector  $\gamma$ , upon setting  $\theta_i = -\operatorname{Re}(e^{-i\psi} Z_\tau(\gamma_i))$  with  $\psi$  s.t.  $\operatorname{Im}(e^{-i\psi} Z_\tau(\gamma_i)) > 0$ .
- For fixed **FI parameters**  $\theta \in \mathbb{R}^{Q_0}$ , a representation of  $\dim \gamma$  is  $\theta$ -semi-stable iff  $(\theta, \gamma') \leq (\theta, \gamma)$  for any subrepresentation.
- In the quiver context, there is a notion of **attractor stability condition** (aka self-stability condition) [*Manschot BP Sen'13; Bridgeland'16*]

$$(\theta_\star(\gamma), \gamma') = \langle \gamma', \gamma \rangle := \sum_{a:i \rightarrow j} (n'_i n_j - n'_j n_i)$$

The (quiver) attractor invariant is defined as  $\Omega_\star(\gamma) := \Omega_{\theta_\star(\gamma)}(\gamma)$

# The Flow Tree formula for quivers

- In [Alexandrov BP'18], we conjectured a precise version of SAFC which expresses  $\bar{\Omega}_\theta(\gamma)$  in terms of the attractor invariants:

$$\bar{\Omega}_\theta(\gamma) = \sum_{\gamma = \sum \gamma_i} \frac{g_\theta(\{\gamma_i\})}{\text{Aut}(\{\gamma_i\})} \prod_i \bar{\Omega}_*(\gamma_i)$$

The coefficients  $g_\theta(\{\gamma_i\})$  involve a sum over **rooted binary trees**, whose edges are embedded in  $\mathbb{R}^{Q_0}$  along straight lines  $\theta_0 + \lambda\theta_*(\gamma_e)$ , which are the analogue of attractor flows.

- The sum is manifestly **finite**, since  $\gamma_i$  lie in the positive cone  $\mathbb{Z}_+^{Q_0}$ .
- The formula was proven mathematically in [Argüz Bousseau'21] using the formalism of **scattering diagrams**.

# Flow tree formula from scattering diagrams

- For any quiver with potential  $(Q, W)$ , the scattering diagram  $\mathcal{D}_Q$  is the set of **real codimension-one rays**  $\{\mathcal{R}(\gamma), \gamma \in \mathbb{Z}^{Q_0}\}$  defined by

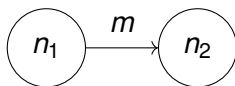
$$\mathcal{R}(\gamma) = \{\theta \in \mathbb{R}^{Q_0} : (\theta, \gamma) = 0, \bar{\Omega}_\theta(\gamma) \neq 0\}$$

- Each point along  $\mathcal{R}(\gamma)$  is endowed with an **automorphism of the quantum torus algebra**,

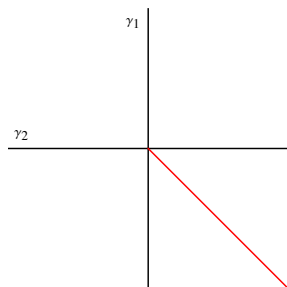
$$\mathcal{U}_\theta(\gamma) = \exp\left(\frac{\bar{\Omega}_\theta(\gamma)}{y^{-1}-y} \mathcal{X}_\gamma\right), \quad \mathcal{X}_\gamma \mathcal{X}_{\gamma'} = (-y)^{\langle \gamma, \gamma' \rangle} \mathcal{X}_{\gamma+\gamma'}$$

- The WCF ensures that the diagram is **consistent**: for any generic closed path  $\mathcal{P} : t \in [0, 1] \in \mathbb{R}^{Q_0}$ ,  $\prod_i \mathcal{U}_{\theta(t_i)}(\gamma_i)^{\epsilon_i} = 1$  [Bridgeland'16]
- A consistent scattering diagram is uniquely determined from the initial rays  $\mathcal{R}_*(\gamma)$ , defined as those which contain  $\theta_*(\gamma)$ .
- The Flow Tree Formula of [Alexandrov BP'18] determines the indices of outgoing rays produced by scattering initial rays [Argüz Bousseau '20].

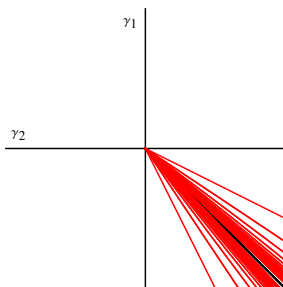
# Scattering diagram for Kronecker quiver



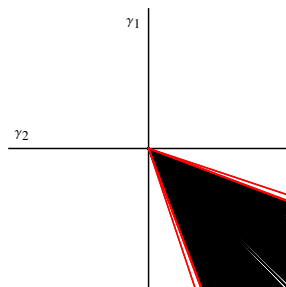
$$\theta_1 > 0, \theta_2 < 0 : \quad \dim \mathcal{M}_\theta(\gamma) = mn_1n_2 - n_1^2 - n_2^2 + 1$$



$m=1$



$m=2$

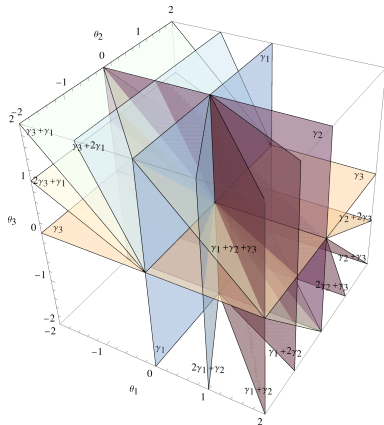


$m=3$



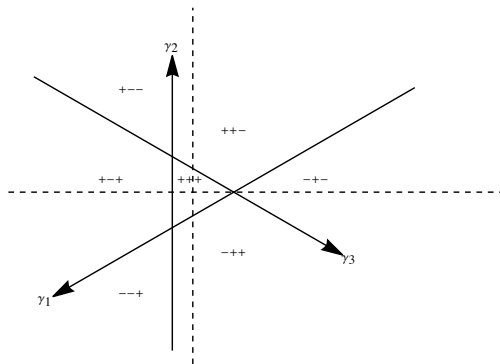
# Attractor invariants for $K_{\mathbb{P}^2}$

- By studying expected dimension of the moduli space of semi-stable representations  $\mathcal{M}_\theta(\gamma)$ , [Beaujard BP Manschot'20] conjectured that **the attractor index  $\Omega_*(\gamma)$  vanishes unless for  $\gamma = \gamma_i$  or  $\gamma = k(\gamma_1 + \gamma_2 + \gamma_3)$** . This is now a theorem [Bousseau Descombes Le Floch BP'22].



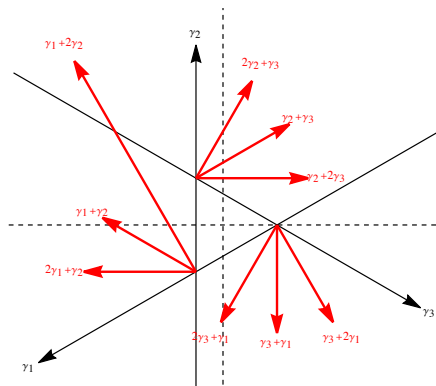
# A 2D slice of the orbifold scattering diagram

Let  $\mathcal{D}_o$  be the restriction of  $\mathcal{D}_Q$  to the hyperplane  $\theta_1 + \theta_2 + \theta_3 = 1$ :



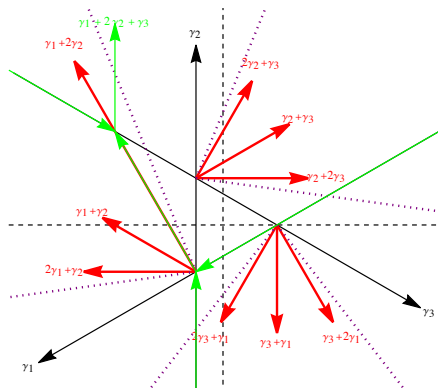
# A 2D slice of the orbifold scattering diagram

Let  $\mathcal{D}_o$  be the restriction of  $\mathcal{D}_Q$  to the hyperplane  $\theta_1 + \theta_2 + \theta_3 = 1$ :



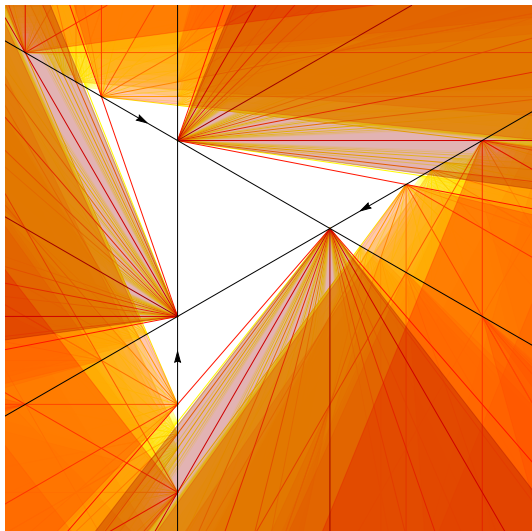
# A 2D slice of the orbifold scattering diagram

Let  $\mathcal{D}_o$  be the restriction of  $\mathcal{D}_Q$  to the hyperplane  $\theta_1 + \theta_2 + \theta_3 = 1$ :



# A 2D slice of the orbifold scattering diagram

The full scattering diagram  $\mathcal{D}_Q$  includes regions with dense set of rays:



# Scattering diagrams on triangulated categories

- For a general triangulated category  $\mathcal{C}$ , define the scattering diagram  $\mathcal{D}_\psi(\mathcal{C})$  as the set of codimension-one loci in  $\text{Stab } \mathcal{C}$ ,

$$\mathcal{R}_\psi(\gamma) = \left\{ \sigma : \arg Z(\gamma) = \psi + \frac{\pi}{2}, \bar{\Omega}_Z(\gamma) \neq 0 \right\}$$

equipped with (a suitable regularization of) the automorphism

$$\mathcal{U}_\sigma(\gamma) = \exp \left( \frac{\bar{\Omega}_\sigma(\gamma)}{y^{-1}-y} \mathcal{X}_\gamma \right) = \text{Exp} \left( \frac{\Omega_\sigma(\gamma)}{y^{-1}-y} \mathcal{X}_\gamma \right)$$

- The WCF ensures that the diagram  $\mathcal{D}_\psi$  is still locally consistent at each codimension-two intersection.

# Flow trees from scattering diagrams

- To see the relation to SAFC, note that for any local CY threefold, the central charge  $Z_z(\gamma)$  is holomorphic in  $z^a$ , hence **its phase is constant along the flow**  $\frac{dz^a}{d\mu} = -g^{a\bar{b}}\partial_{\bar{b}}|Z_z(\gamma)|^2$ :

$$\frac{1}{2} \frac{d}{d\mu} \log \frac{Z(\gamma)}{\bar{Z}(\gamma)} = -\frac{1}{2} \partial_a Z(\gamma) g^{a\bar{b}} \partial_{\bar{b}} \bar{Z}(\gamma) + \frac{1}{2} \partial_a Z(\gamma) g^{a\bar{b}} \partial_{\bar{b}} \bar{Z}(\gamma) = 0$$

Moreover,  $|Z_z(\gamma)|^2$  has no local minima so **the only attractor points are conifold points** with  $Z_z(\gamma_i) = 0$ .

- Thus, the restriction of  $\mathcal{R}_\psi(\gamma)$  to the physical slice is preserved by the attractor flow. Moreover, the flow can only split when  $\mathcal{R}(\gamma_L)$  and  $\mathcal{R}(\gamma_R)$  intersect, and end on an initial ray  $\mathcal{R}_\psi(\gamma_i)$ .
- In complex dimension one, attractor flow lines and scattering rays coincide. Attractor flow trees are subsets of  $\mathcal{D}_\psi$  which produce an outgoing ray  $\mathcal{R}_\psi(\gamma)$  with desired charge  $\gamma$ , passing through the desired point  $z$ .

# Large volume scattering diagram

- The scattering diagram  $\mathcal{D}_\psi^{\text{LV}}$  along the large volume slice

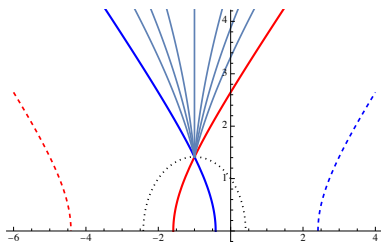
$$Z_{(s,t)}^{\text{LV}} = -\frac{1}{2}r(s+it)^2 + d(s+it) - ch_2$$

was determined for  $\psi = 0$  in [Bousseau'19], using a different set of coordinates. The construction extends to any  $\psi$  by just mapping  $(s, t) \mapsto (s - t \tan \psi, t / \cos \psi)$ .

- Since  $\text{Re}Z(\gamma) = \frac{1}{2}r(t^2 - s^2) + ds - ch_2$ , each ray  $\mathcal{R}_0(\gamma)$  is contained in a **branch of hyperbola** asymptoting to  $t = \pm(s - \frac{d}{r})$  for  $r \neq 0$ , or vertical a line when  $r = 0$ . Walls of marginal stability  $\mathcal{W}(\gamma, \gamma')$  are **half-circles** centered on real axis.



# Large volume scattering diagram

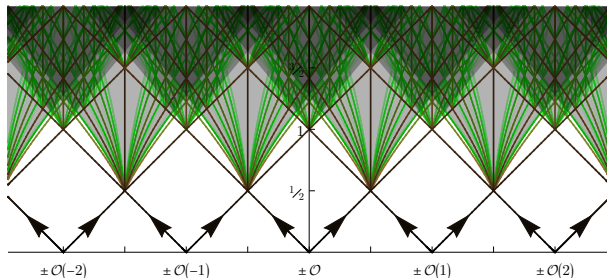


It is useful to think of  $\mathcal{R}(\gamma)$  as the worldline of a fictitious particle of charge  $r$ , mass  $M^2 = \frac{1}{2}d^2 - rch_2$  moving in a constant electric field:

- The particle travels inside the forward light-cone
- the 'electric potential'  $\varphi_s(\gamma) = 2(d - sr) = 2\text{Im}Z_\gamma/t$  increases along the flow.

# Large volume scattering diagram

- Initial rays correspond to  $\mathcal{O}(m)$  and  $\mathcal{O}(m)[1]$ , with charge  $\gamma_m = \pm[1, m, \frac{1}{2}m^2]$ , emanating from  $(s, t) = (m, 0)$  on the boundary where  $Z_{(s,t)}^{LV}(\gamma_m) = 0$ . [Bousseau'19]



- Physically, the BPS spectrum along the large volume slice originates from bound states of fluxed D4-branes and anti-D4 branes.

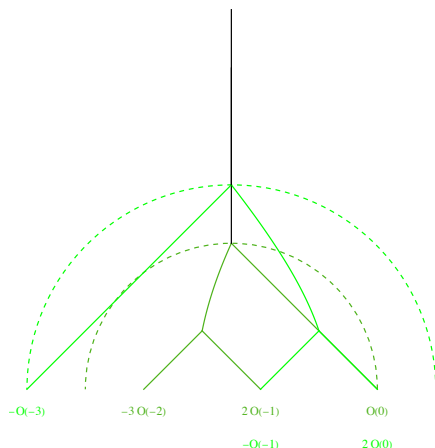
# SAFC holds along large volume slice

- The first scatterings occur after a time  $t \geq \frac{1}{2}$ , after each constituent  $k_i \mathcal{O}(m_i)$  has moved by  $|\Delta s| \geq \frac{1}{2}$ , by which time  $\varphi_s(\gamma_i) \geq |k_i|$ .
- Since  $\varphi_s(\gamma)$  is additive at each vertex, this gives a bound on the number and charges of constituents contributing to  $\Omega_{(s,t)}(\gamma)$ :

$$\sum_i k_i [1, m_i, \frac{1}{2} m_i^2] = \gamma, \quad s - t \leq m_i \leq s + t, \quad \sum |k_i| \leq \varphi_s(\gamma)$$

- Thus, SAFC holds along the large volume slice !

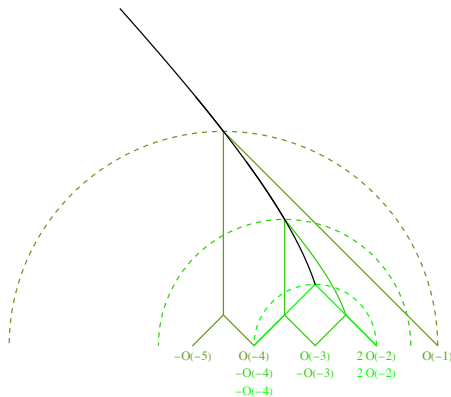
# Flow trees for $\gamma = [0, 4, 1)$



- $\{\{-3\mathcal{O}(-2), 2\mathcal{O}(-1)\}, \mathcal{O}\}$ :  
 $3\mathcal{O}(-2) \rightarrow 2\mathcal{O}(-1) \oplus \mathcal{O} \rightarrow E$   
 $K_3(2, 3)K_{12}(1, 1) \rightarrow -156$
- $\{-\mathcal{O}(-3), \{-\mathcal{O}(-1), 2\mathcal{O}\}\}$ :  
 $\mathcal{O}(-3) \oplus \mathcal{O}(-1) \rightarrow 2\mathcal{O} \rightarrow E$   
 $K_3(1, 2)K_{12}(1, 1) \rightarrow -36$

Total:  $\Omega_\infty(\gamma) = -192 = GV_4^{(0)}$

# Flow trees for $\gamma = [1, 0, -3]$

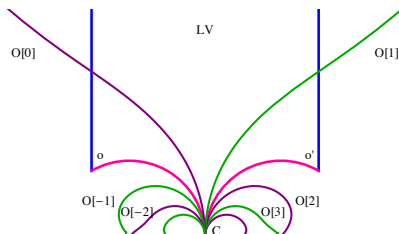


- $\{\{-\mathcal{O}(-5), \mathcal{O}(-4)\}, \mathcal{O}(-1)\}$   
 $\mathcal{O}(-5) \rightarrow \mathcal{O}(-4) \oplus \mathcal{O}(-1) \rightarrow E$   
 $K_3(1, 1)^2 \rightarrow 9$
- $\{\{-\mathcal{O}(-4), \mathcal{O}(-3)\},$   
 $\{-\mathcal{O}(-3), 2\mathcal{O}(-2)\}\}$   
 $\mathcal{O}(-4) \oplus \mathcal{O}(-3) \rightarrow$   
 $\mathcal{O}(-3) \oplus 2\mathcal{O}(-2) \rightarrow E$   
 $K_3(1, 1)^2 K_3(1, 2) \rightarrow 27$
- $\{-\mathcal{O}(-4), 2\mathcal{O}(-2)\}$   
 $\mathcal{O}(-4) \rightarrow 2\mathcal{O}(-2) \rightarrow E$   
 $K_6(1, 2) \rightarrow 15$

Total:  $\Omega_\infty(\gamma) = 51 = \chi(\text{Hilb}_4 \mathbb{P}^2)$

# Exact scattering diagram

- The scattering diagram  $\mathcal{D}_\psi^\Pi$  along the physical slice should interpolate between  $\mathcal{D}_\psi^{\text{LV}}$  around  $\tau = i\infty$  and  $\mathcal{D}_o$  around  $\tau = \tau_o$ , and be invariant under the action of  $\Gamma_1(3)$ .
- Under  $\tau \mapsto \frac{\tau}{3n\tau+1}$  with  $n \in \mathbb{Z}$ ,  $\mathcal{O} \mapsto \mathcal{O}[n]$ . Hence there is a doubly infinite family of initial rays emitted at  $\tau = 0$ , associated to  $\mathcal{O}[n]$ .



- Similarly, there must be an infinite family of initial rays coming from  $\tau = \frac{p}{q}$  with  $q \not\equiv 0 \pmod{3}$ , corresponding to  $\Gamma_1(3)$ -images of  $\mathcal{O}$ , where an object denoted by  $\mathcal{O}_{p/q}$  becomes massless.

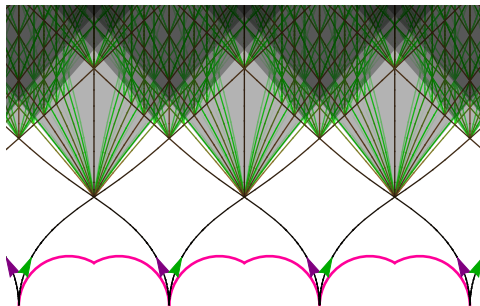
# Massless objects at conifold points

$\tau$	$g$	$\gamma_C$	$\Delta(\gamma_C)$	$\mathcal{O}_{p/q}$
0	1	[1, 0, 1)	0	$\mathcal{O}$
1/5	$U^2 T^{-1}$	-[5, 1, 6)	3/25	$E \rightarrow \Omega(2)[-1] \rightarrow \mathcal{O}^{\oplus 3}[2]$
1/4	$UT$	[4, 1, 6)	-3/32	$E \rightarrow \mathcal{O}(1) \rightarrow \mathcal{O}^{\oplus 3}[3]$
2/5	$UT^{-2}$	-[5, 2, 6)	12/25	$E \rightarrow \mathcal{O}(-2) \rightarrow \mathcal{O}^{\oplus 6}$
3/7	$UT^{-1}VT$	[7, 3, 10)	15/49	$E \rightarrow \Omega(0)[1] \rightarrow \mathcal{O}^{\oplus 9}[1]$
1/2	$TVT$	-[2, 1, 3)	3/8	$\Omega(2)[1]$
4/7	$TVTUT^{-1}$	[7, 4, 12)	15/49	$\mathcal{O}(1)^{\oplus 9}[-1] \rightarrow \Omega(4)[-1] \rightarrow E$
3/5	$TVT^2$	-[5, 3, 8)	12/25	$\mathcal{O}(1)^{\oplus 6} \rightarrow \mathcal{O}(3) \rightarrow E$
3/4	$TVT^{-1}$	[4, 3, 10)	-3/32	$\mathcal{O}(1)^{\oplus 3}[-3] \rightarrow \mathcal{O}(0) \rightarrow E$
4/5	$TV^2T$	-[5, 4, 12)	3/25	$\mathcal{O}(1)^{\oplus 3}[-2] \rightarrow \Omega(2)[1] \rightarrow E$
1	$T$	[1, 1, 3)	0	$\mathcal{O}(1)$

$$T : \tau \mapsto \tau + 1; \quad U : \tau \mapsto 1/(3\tau + 1); \quad V = U^{-1}$$

# Exact scattering diagram for small $\psi$

- For  $|\psi|$  small enough, the only rays which reach the large volume region are those associated to  $\mathcal{O}(m)$  and  $\mathcal{O}(m)[1]$ . Thus, the scattering diagram  $\mathcal{D}_\psi^\square$  is isomorphic to  $\mathcal{D}_0^{LV}$  inside  $\mathcal{F}$  and its translates:





# Scattering diagram in affine coordinates

- To see this, one can map both of them to the plane

*Bousseau'19*

$$x = \frac{\operatorname{Re}(e^{-i\psi} T)}{\cos \psi}, \quad y = -\frac{\operatorname{Re}(e^{-i\psi} T_D)}{\cos \psi},$$

such that  $\mathcal{R}_\psi(\gamma)$  becomes a line segment  $rx + dy - ch_2 = 0$ .

- The initial rays  $\mathcal{R}_{\mathcal{O}(m)}$  are tangent to the parabola  $y = -\frac{1}{2}x^2$  at  $x = m$ , but the origin of each ray is shifted to  $x = m + \mathcal{V} \tan \psi$  where  $\mathcal{V}$  is the quantum volume

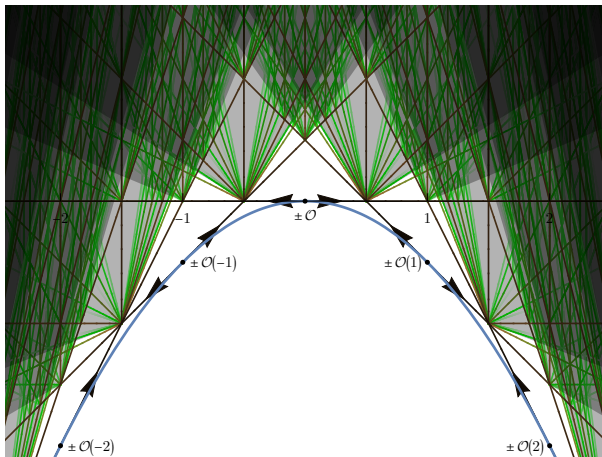
$$\mathcal{V} = \operatorname{Im} T(0) = \frac{27}{4\pi^2} \operatorname{Im} \left[ \operatorname{Li}_2(e^{2\pi i/3}) \right] \simeq 0.463$$

- The topology of  $\mathcal{D}_\psi^\square$  jumps at a discrete set of rational values

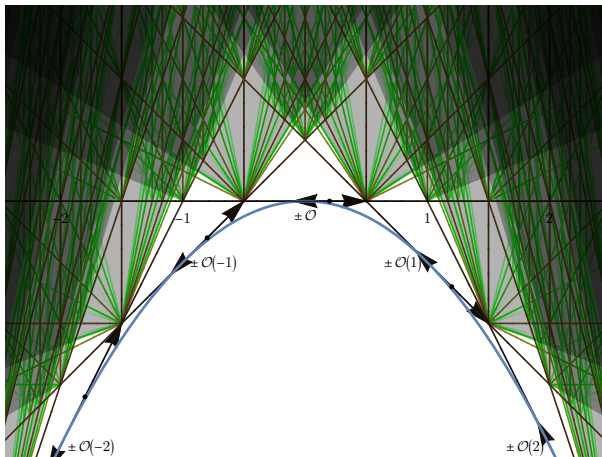
$$\mathcal{V} \tan \psi \in \left\{ \frac{F_{2k} + F_{2k+2}}{2F_{2k+1}}, k \geq 0 \right\} = \left\{ \frac{1}{2}, 1, \frac{11}{10}, \frac{29}{26}, \frac{19}{17}, \dots \right\}$$

and a dense set of values in  $[\frac{\sqrt{5}}{2}, +\infty)$  where secondary rays pass through a conifold point.

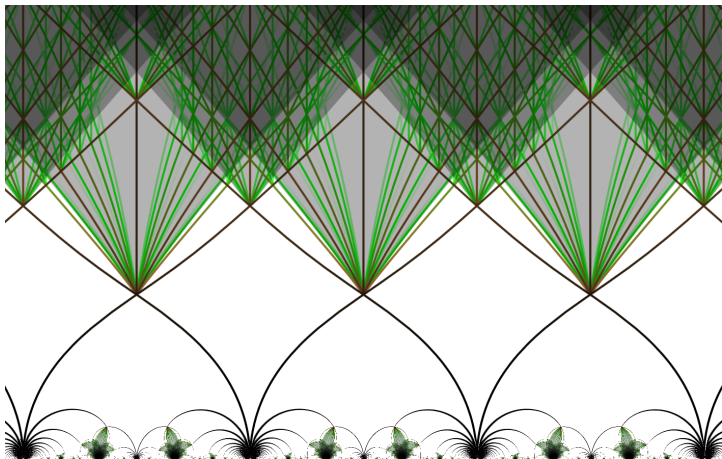
# Affine scattering diagram, $\psi = 0$



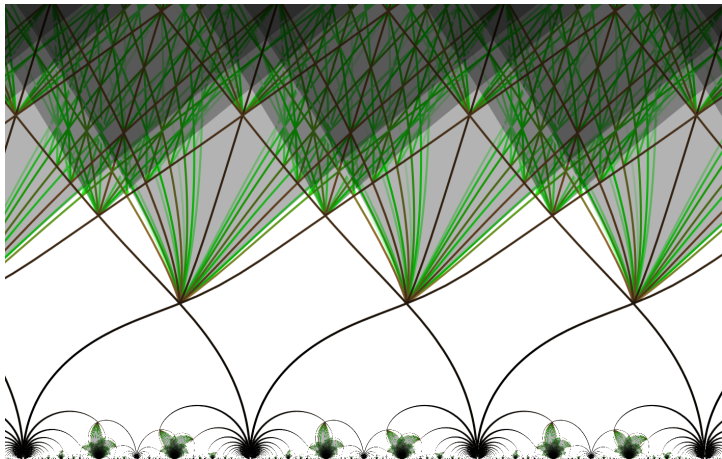
# Affine scattering diagram, $|\mathcal{V} \tan \psi| < 1/2$



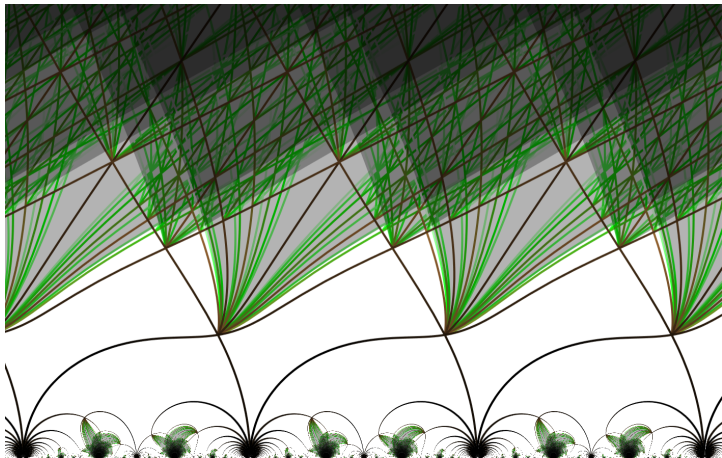
# Exact scattering diagram, $\psi = 0$



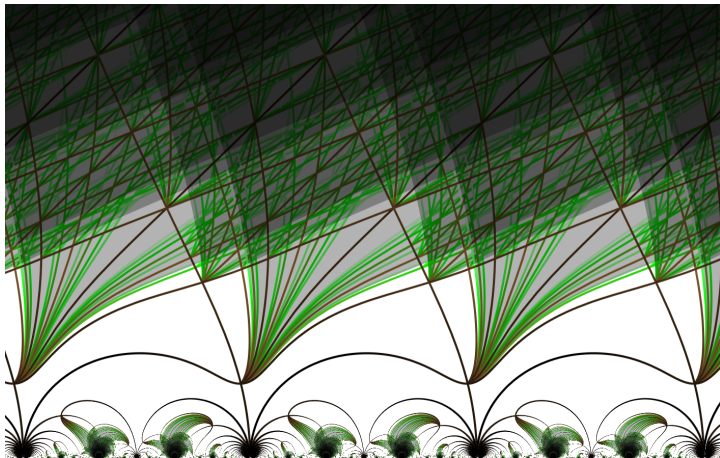
# Exact scattering diagram, $\psi = 0.3$



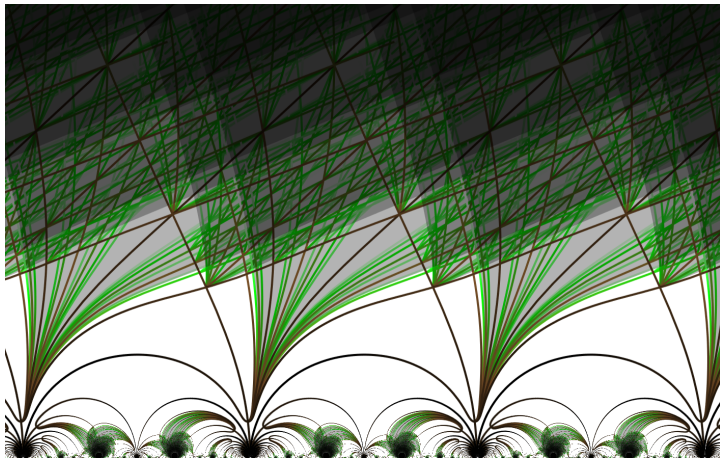
# Exact scattering diagram, $\psi = 0.6$



# Exact scattering diagram, $\psi = 0.8$

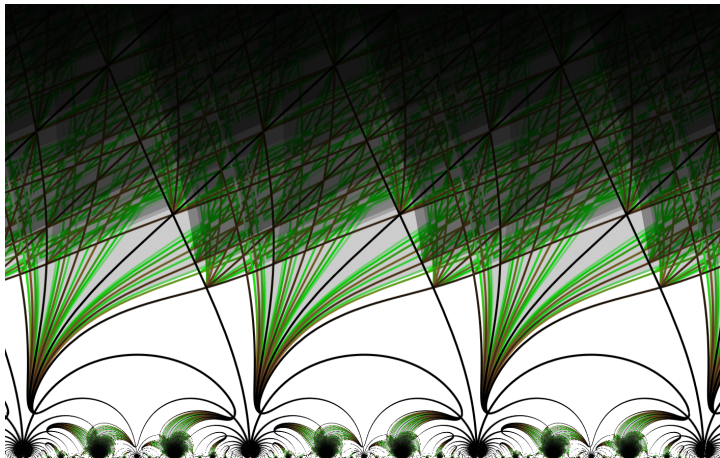


# Exact scattering diagram, $\psi = 0.824$

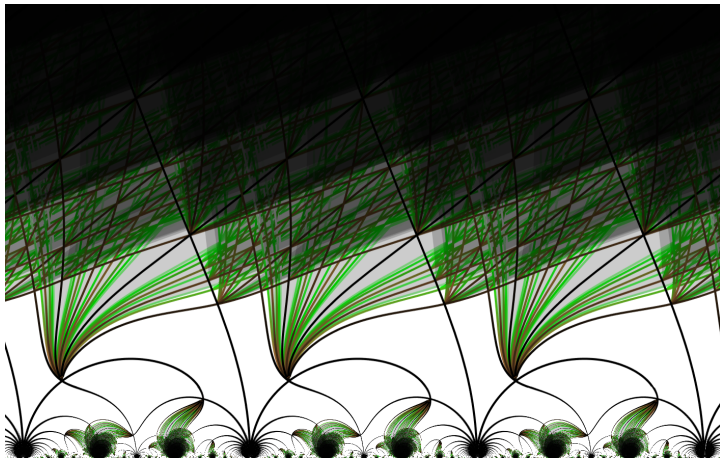




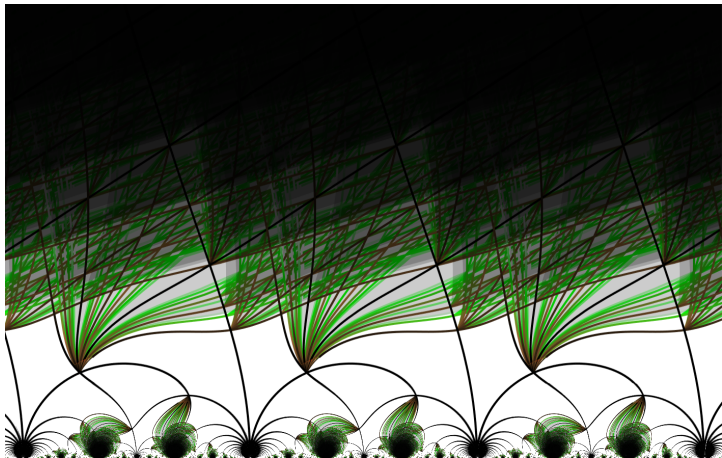
# Exact scattering diagram, $\psi = 0.825$



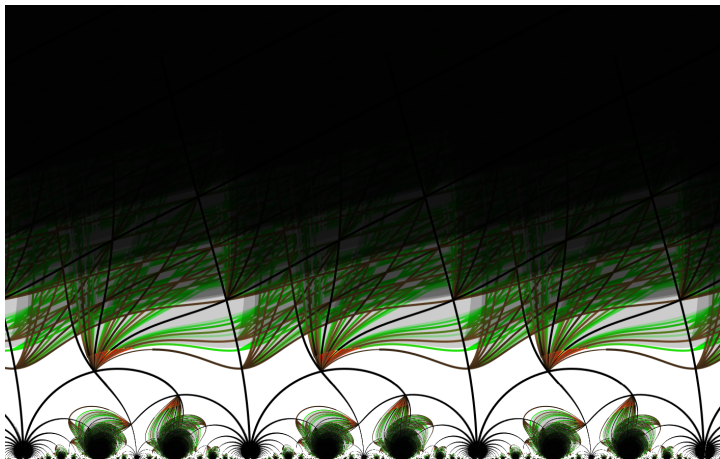
# Exact scattering diagram, $\psi = 0.9$



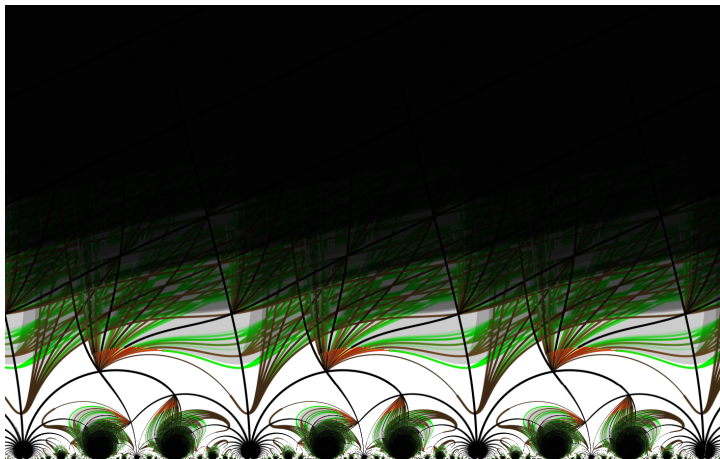
# Exact scattering diagram, $\psi = 1$



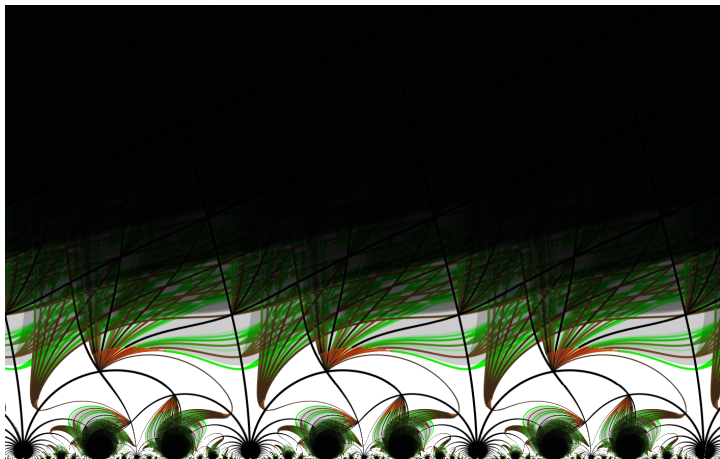
# Exact scattering diagram, $\psi = 1.1$



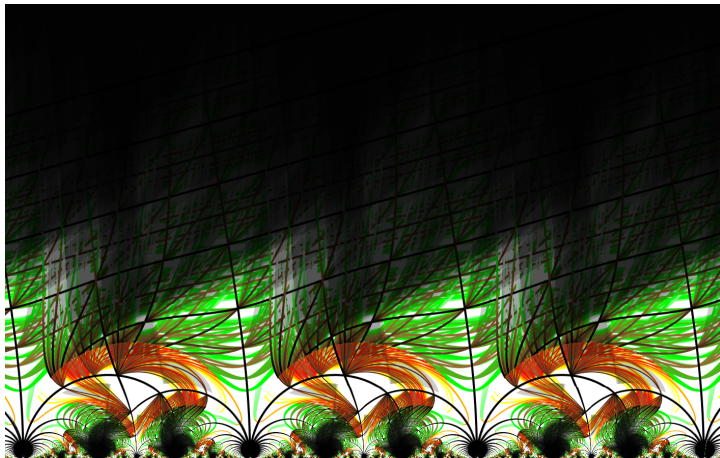
# Exact scattering diagram, $\psi = 1.137$



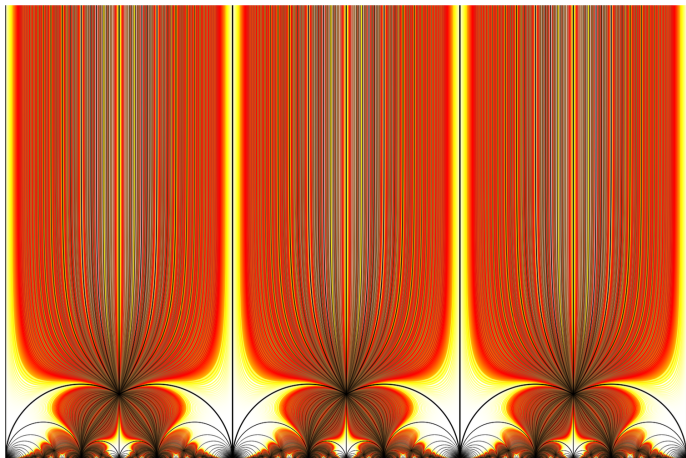
# Exact scattering diagram, $\psi = 1.139$



# Exact scattering diagram, $\psi = 1.3$



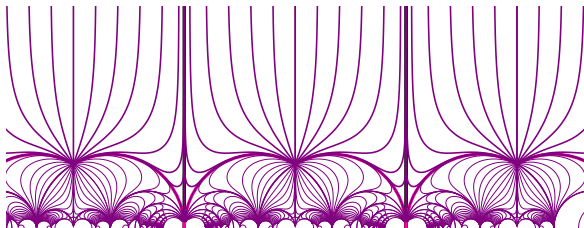
# Exact scattering diagram, $\psi = \pi/2$





# Exact scattering diagram for $\psi = \pm \frac{\pi}{2}$

- For  $\psi = \pm \frac{\pi}{2}$ , the geometric rays  $\{\text{Im}Z_\tau(\gamma) = 0\}$  coincide with lines of constant  $s = \frac{\text{Im}T_D}{\text{Im}T} = \frac{d}{r}$ , independent of  $\text{ch}_2$ :

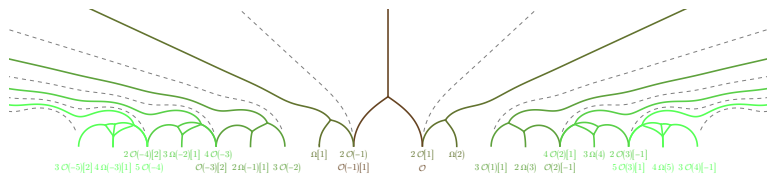


- Hence, there is no wall-crossing between  $\tau_0$  and  $\tau = i\infty$  when  $-1 \leq \frac{d}{r} \leq 0$ , explaining why the Gieseker index  $\Omega_\infty(\gamma)$  agrees with the quiver index  $\Omega_c(\gamma)$  in the anti-attractor chamber.

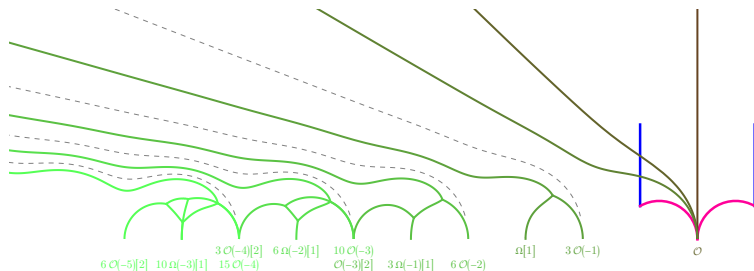
*Douglas Fiol Romelsberger'00, Beaujard BP Manschot'20*

# Case studies

$$\gamma = [0, 1, 1] = \text{ch } \mathcal{O}_C: \Omega_{t \gg 1} = K_3(1, 2)K_3(1, 3)^{n-1} = y^2 + 1 + 1/y^2$$

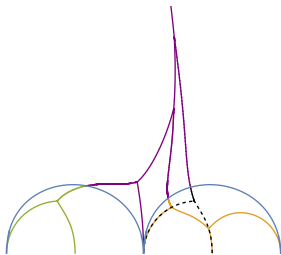


$$\gamma = [1, 0, 1] = \text{ch } \mathcal{O}: \Omega_{t \gg 1} = K_3(1, 3) \dots K_3(1, 3n) = 1$$



# SAFC along the physical slice

- In general, trees reaching the large volume region have a two-stage structure, with initial rays from a finite set of exceptional collections  $\{E_1(m_i), E_2(m_i), E_3(m_i)\}$ , which scatter in the vicinity of orbifold points  $\tau = \tau_0 + m_i$ , and then further interact in the large volume region.



- The SFAC is proved by analyzing the possible leaves, defining a monotonic cost function  $\varphi$  and classifying allowed trees...

# Conclusion - outlook

- The scattering diagram is the proper mathematical framework for the attractor flow tree formula in the case of local CY3. This is because  $Z(\gamma)$  is holomorphic on  $\mathcal{M}_K$ , so the gradient flow preserves the phase  $\arg Z(\gamma)$ .
- This provides an effective way of computing (unframed) BPS invariants in any chamber, and a natural decomposition into elementary constituents. Is this mathematically meaningful ? Does it help e.g. in understanding modularity ?
- It would be interesting to extend this description to other toric CY3, such as local del Pezzo surfaces.
- For compact CY3,  $Z(\gamma) = e^{K/2} Z_{\text{hol}}(\gamma)$  is not longer holomorphic, so  $\arg Z(\gamma)$  is not constant along the flow. Can one establish the Split Attractor Flow Tree formula in such context ?

Thanks for your attention !

